The Reactivity of Surface Oxygen Phases on Pd(100) Toward Reduction by CO

G. Zheng and E. I. Altman*

Department of Chemical Engineering, Yale University, New Haven, Connecticut 06520

Received: September 5, 2001; In Final Form: November 19, 2001

The reactivities of surface oxygen phases on Pd(100) toward reduction by CO were characterized using temperature-programmed desorption and reaction (TPD, TPR), isothermal kinetic measurements, low energy electron diffraction (LEED), and scanning tunneling microscopy (STM). When CO was exposed to high oxygen coverages where bulk PdO and a ($\sqrt{5} \times \sqrt{5}$)R27° oxygen-induced reconstruction exist on the surface, a lag was observed before any CO_2 was produced. The CO_2 formation rate then increased before falling as the oxygen was depleted. LEED showed that the rate increased as (2 × 2) domains replaced the ($\sqrt{5} \times \sqrt{5}$)R27° structure on the surface indicating that the lag was due to the slow reduction of ($\sqrt{5} \times \sqrt{5}$)R27° domains. In contrast, LEED showed that a lower oxygen coverage (5 × 5) reconstruction is immediately destroyed by exposure to CO. Therefore, the results indicated that the more oxidized ($\sqrt{5} \times \sqrt{5}$)R27° surface and PdO are relatively unreactive toward CO. Further, the temperature dependence of the reduction rate and the TPR results suggested that the inactivity of these surfaces is due to their inability to strongly adsorb CO. STM movies recorded while CO was exposed to oxygen-covered surfaces showed that the (2 × 2) domains were not reduced until the ($\sqrt{5} \times \sqrt{5}$)R27° structure was completely removed from the surface. This indicated that oxygen from neighboring ($\sqrt{5} \times \sqrt{5}$)R27° domains replenished the oxygen in the reactive (2 × 2) domains lost by reaction with CO; thus oxygen transport between these phases is rapid. Similarly, the sensitivity of the lag in the CO_2 production to very small changes in the amount of bulk PdO could be explained in terms of rapid transport of oxygen from PdO to ($\sqrt{5} \times \sqrt{5}$)R27° domains preventing their reduction to more reactive (2 × 2) structures until all the PdO was removed.

I. Introduction

Palladium has attracted considerable interest as a catalyst for the complete oxidation of hydrocarbons in automotive exhausts[1−3] and is the only suitable catalyst for the catalytic combustion of methane in ultralow NO_x advanced gas turbines.[4−6] Palladium-catalyzed oxidation reactions exhibit unusual phenomena such as kinetic oscillations in CO and CH_4 oxidation rates and an extreme sensitivity of the catalyst activity to its history.[5,7−13] Since Pd can exist in bulk metallic and oxidic states under reaction conditions, it has been suggested that transitions between these states account for these phenomena.[4,5,7,11,14] Surface science studies, however, have shown that oxygen can exist on Pd surfaces in many different states, including several that are intermediate between a chemisorbed layer atop the metal surface and PdO.[15−22] This paper addresses the reactivity of the different surface oxygen phases on Pd(100) toward CO oxidation.

Palladium oxidation is a complex process. On Pd(100), oxidation proceeds through four stages involving up to six distinct surface oxygen phases.[16,19−21] The first stage is dissociative adsorption to form a simple overlayer. Up to 0.25 ML, the oxygen atoms form a p(2 × 2) chemisorbed overlayer that desorbs in a peak at 800 K. Above 0.25 ML, the p(2 × 2) layer coexists with a c(2 × 2) layer. In the second stage, Pd atoms ejected onto the terraces diffuse across the surface and either nucleate islands or attach to preexisting steps.[16] The surface periodicity does not change during this stage and so the diffusing Pd atoms have been attributed to atoms displaced by oxygen filling subsurface sites. After island growth stops the surface reconstructs in the third stage. Above 400 K, a ($\sqrt{5} \times \sqrt{5}$)-R27° structure is observed. Tensor low energy electron diffraction (LEED) studies indicate that this reconstruction is due to a rumpled PdO(001)-like surface;[23] scanning tunneling microscopy (STM) results support this assignment.[16] At lower temperatures a (5 × 5) reconstruction is observed. In the third stage, a sharp oxygen desorption peak appears at 650 K and shifts above 700 K at saturation. These temperatures are much lower than the 800 K observed for chemisorption but higher than that expected for bulk PdO dissociation, suggesting a Pd−O bond strength intermediate between chemisorbed oxygen and bulk PdO.[16] In the fourth stage, the surface roughens and a desorption peak associated with bulk PdO dissociation appears.[16] The oxidation of the other low-index surfaces is just as complex. The (111) surface also exhibits two distinct oxygen-induced reconstructions before bulk PdO forms,[15] and it has been suggested that oxygen can fill subsurface sites on Pd(110).[22] Thus studying the reactivity of surface oxygen phases on Pd(100) will provide general insight into the reactivity of Pd surfaces under oxidizing conditions.

The oxidation of CO over Pd(100) has previously been studied by coadsorbing oxygen and CO at 100 K and then performing temperature-programmed reaction (TPR).[24] Carbon dioxide was observed in three peaks: at 420 K, 360 K, and between 100 and 310 K. There was no evidence of molecularly adsorbed CO_2 or carbonate intermediates and so the CO_2 peaks reflected the CO oxidation kinetics on the surface. In this work, the oxygen coverage was limited to the chemisorption regime. In other work, CO oxidation kinetics over Pd(100) have been measured at pressures up to 100 Torr.[25,26] These studies,

* Corresponding author. Fax (203) 432−4387. E-mail: eric.altman@yale.edu.

10.1021/jp013395x CCC: $22.00
Published on Web 01/15/2002

however, focused on the regime where the surface is predominantly covered by CO and the reaction is limited by CO blocking oxygen adsorption. Thus the relative reactivity of the different surface oxygen phases on Pd(100) toward CO remains an open question.

In this paper it will be shown that chemisorbed oxygen is far more reactive toward CO than the PdO(001)-like reconstructed surface which in turn is more reactive than bulk PdO. In addition, the results indicate that oxygen readily moves between bulk PdO and the reconstructed phases so that as oxygen is removed from the reconstructed surface it is replenished by oxygen from PdO. Similarly, oxygen rapidly moves from the reconstructed phases to the (2×2) phases. Finally, it will be shown that the reaction rate depends not only on the oxygen coverage but also on how that coverage is reached.

II. Experimental Section

Experiments were performed using a UHV system equipped with a quadrupole mass spectrometer, a double pass cylindrical mirror analyzer for Auger electron spectroscopy (AES), an ion gun for sputtering, LEED optics, and a high-speed variable-temperature scanning tunneling microscope.[27] Diffraction patterns were recorded using a CCD camera and a frame grabber board; LEED movies were recorded by streaming the images to the computer hard disk. Mass spectrometry and TPD were performed line-of-sight with the sample positioned within a few centimeters of the ionizer of the mass spectrometer. Mounting and preparation of the Pd(100) surface has been described previously.[16]

Because the sticking coefficient for the oxidants can be low, the oxidants were dosed using directed dosers. The system was equipped with two such dosers, one directed at the tunnel junction of the microscope, the other at the manipulator. The manipulator doser gave effective pressures 45 times the background pressure while the STM doser had an enhancement factor of 5.[15] The data presented in this paper have taken these factors into account. Carbon monoxide was dosed by simply increasing the CO background pressure. Pressures were measured using two ionization gauges, one located just above the ion pump and the other at the manipulator level. The readings from the two gauges agreed within 5% when CO was leaked into the chamber through either of the two leak valves on the system. The default controller calibrations for N_2 were used for both gauges; however, the sensitivity factor for CO relative to N_2 is 1.02 and so this did not introduce significant errors into the pressure measurement.[28]

Both O_2 and NO_2 were used as oxidants. On Pd surfaces, NO_2 dissociates yielding atomic oxygen and NO.[18] At 500 K the NO rapidly desorbs and so NO_2 exposure yields the same TPD peaks and LEED patterns as O_2.[15,16,18] Molecular oxygen, however, is far less reactive than NO_2 (up to a factor of 100),[16] and so NO_2 was used in many of the experiments. Oxygen coverages were estimated on the basis of TPD work that yielded oxygen uptake curves as a function of O_2 and NO_2 exposure at different temperatures, the curve for NO_2 is provided in Figure 1.[16] In this study, it was assumed that saturating the sharp desorption peak at 700 K corresponded to completely covering the surface with a $(\sqrt{5} \times \sqrt{5})$R27° structure that has an ideal coverage of 0.8 ML, where 1 ML is defined as 1 atom per surface Pd atom on an unreconstructed Pd(100) surface. This calibration was supported by STM images that showed a surface covered by $(\sqrt{5} \times \sqrt{5})$R27° domains and small amounts PdO clusters at the highest exposures, consistent with the maximum coverage of 0.9 ML indicated in Figure 1. In earlier work, Stuve et al. had suggested that saturation of a desorption peak at 800 K corresponds to saturating a $p(2 \times 2)$ structure at 0.25 ML.[24] Using this calibration would increase the coverages by about 20%.

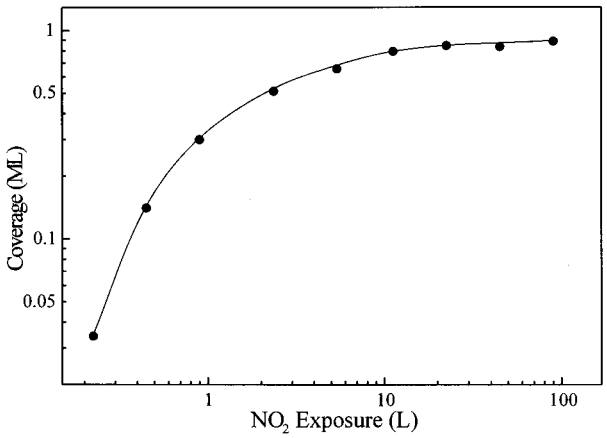

Figure 1. Plot of oxygen uptake versus NO_2 exposure for Pd(100) at 500 K. Data taken from ref 16.

III. Results

a. TPR of Coadsorbed CO and O. Temperature-programmed reaction was performed by dosing with O_2, then exposing the surface to CO at 335 K before ramping the temperature at a rate of 5 K/s. Results are shown in Figure 2 for two initial O_2 exposures: 45 L of O_2 at 340 K in Figure 2a and 45 L of O_2 at 500 K in Figure 2b. At 340 K, 45 L of O_2 exposure results in atomic oxygen adsorbed in $c(2 \times 2)$ and $p(2 \times 2)$ domains.[19,20,24] The oxygen desorbs in a sharp peak at 650 K and a broad peak at 800 K as shown in the O_2 desorption trace for 0 L of CO exposure in Figure 2a. When 0.25 L of CO was exposed to this surface, the 650 K desorption peak was removed but only a very small amount of CO_2 could be observed. When the CO exposure was increased to 0.5 L, the intensity of the 800 K peak decreased and CO_2 could be observed in a peak at 395 K. Finally, a 1 L CO dose completely removed the O, shifted the CO_2 peak to 405 K, and left excess CO on the surface that desorbed at 510 K; the lower temperature CO feature is due to CO_2 cracking.

Previous studies have associated the 800 K desorption peak with O adsorbed in a $p(2 \times 2)$ overlayer,[20,21,24] thus the disappearance of the 650 K peak after exposure to 0.25 L of CO suggests removal of the $c(2 \times 2)$ domains. Since very little CO_2 was observed, the reaction of CO with $c(2 \times 2)$ O must be fast at 335 K. The higher CO exposures produced a CO_2 peak at about 400 K in good agreement with Stuve et al. who attributed a CO_2 peak at 420 K to reaction of CO with $p(2 \times 2)$ islands;[24] the lower temperature seen here can be attributed to the three times slower heating rate used in this study. Finally, the excess CO desorbed at the temperature expected for CO adsorbed on a clean Pd(100) surface.[24]

At 500 K, a 45 L O_2 dose causes the surface to reconstruct into (5×5) and $(\sqrt{5} \times \sqrt{5})$R27° structures. At this exposure, the entire surface is not reconstructed and the (2×2) spots are still visible in the LEED pattern.[16] Compared to adsorption at 340 K, the oxygen coverage was 60% higher. Exposing this surface to CO decreased the intensity of the sharp desorption peak and produced CO_2 in a peak at 375. At 1 L of CO, the results suggest a CO_2 shoulder above 400 K that appears similar to the feature in Figure 2a.

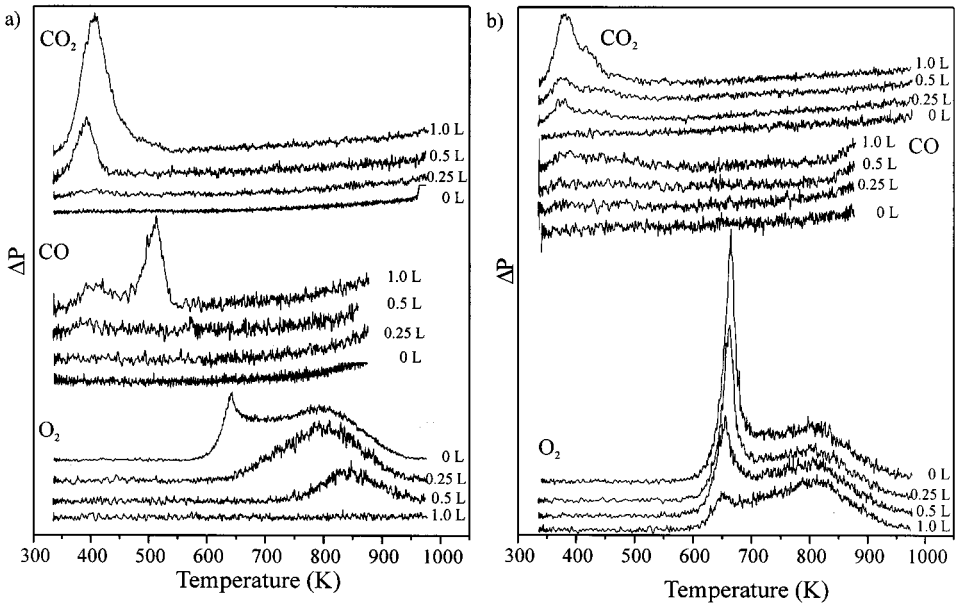

Figure 2. Temperature-programmed reaction traces for O_2 exposure followed by CO exposures of 0, 0.25, 0.5, and 1.0 L. (a) 45 L of O_2 dosed at 340 K. (b) 45 L of O_2 dosed at 500 K.

Stuve et al. also observed a CO_2 peak at roughly 375 K and attributed it to reaction of CO with disordered oxygen islands.[24] The much higher oxygen coverage in this case suggests an alternate origin. The peak could be due to reaction of O with the reconstructed surface. The appearance of the higher temperature CO_2 shoulder then signals the onset of reaction with p(2 × 2) O. Whatever the origin of the peak, comparing Figure 2a and 2b indicates that the reconstruction affects CO oxidation. For O_2 exposure at 340 K, more oxygen is removed per CO molecule exposed to the surface (a factor of 2 at 0.5 L), thus the reconstruction decreases the CO sticking probability. Also, for the 500 K exposure there is no evidence of oxygen removal without also seeing CO_2 in the TPR traces suggesting that little if any reaction takes place at 335 K. Finally, the CO_2 seen at 375 K is different from both the c(2 × 2) oxygen overlayer which reacts at and below 335 K and the p(2 × 2) overlayer which reacts at 400 K.

b. CO Oxidation Kinetics on Oxygen-Covered Pd(100). The dependence of the CO oxidation rate on oxygen coverage was characterized by covering the surface with oxygen and then suddenly increasing the CO pressure while monitoring the CO_2 evolved as a function of time with the mass spectrometer. Figure 3 shows a series of results for temperatures between 400 and 540 K and a CO pressure of 7×10^{-8} Torr. In each of these experiments, the sample was preexposed to 45 L of NO_2 at 500 K which resulted in an oxygen coverage of 0.9 ML according to Figure 1.

The traces in Figure 3 can be viewed in a manner analogous to TPD curves. The integral of the curves is proportional to the initial coverage, and as long as the pumping speed is high, the increase in the CO_2 partial pressure is proportional to the reaction rate.[29] Thus the lag before any CO_2 was observed at 540 K indicates that at this temperature the reaction rate was very slow at the highest coverages. The rate then rose linearly with decreasing coverage until so much oxygen was depleted that the rate fell. This sequence led to the peaked appearance of the curve. As shown in Figure 3, the lag decreased with decreasing temperature and by 450 K was completely gone. At the same time, the peak narrowed and the peak height increased.

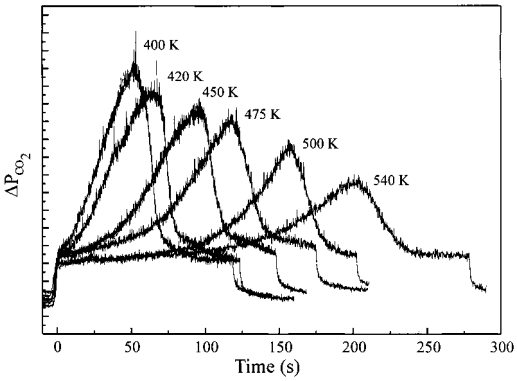

Figure 3. Plots of the rise in CO_2 partial pressure versus time for CO exposed at 7×10^{-8} Torr to Pd(100) preexposed to 45 L of NO_2 at 500 K that leads to an O coverage of 0.9 ML based on Figure 1. The reactions were carried out at the temperatures noted in the figure. The jumps in the CO_2 pressure at $t = 0$ and at the ends of the traces are due to starting and stopping the reaction of CO with the walls of the vacuum chamber as the leak valve was opened and closed.

For the traces in Figure 3, the oxygen coverage θ at any time is given by:

$$(1)\ \theta(t) = \theta_0\left[1 - \frac{\int_0^t \Delta P(s)\,\mathrm{d}s}{\int_0^\infty \Delta P(s)\,\mathrm{d}s}\right]$$

where θ_0 is the initial coverage, ΔP is the increase in the CO_2 pressure, and infinity can be taken as any time after the CO_2 pressure has fallen back to the baseline. In addition, since ΔP is proportional to the CO_2 evolution rate, if the initial coverage is known then the rate can be calculated in units of ML/s of oxygen removed. Thus, using the initial oxygen coverage from the NO_2 uptake curve allows the traces in Figure 3 to be converted into the plots of reaction rate versus coverage shown in Figure 4. The curves in Figure 4 show that the rates were uniformly higher at the lower temperatures and peak at about 0.25 ML. There are some differences between the curves. At and above 500 K, the rate increased linearly with oxygen

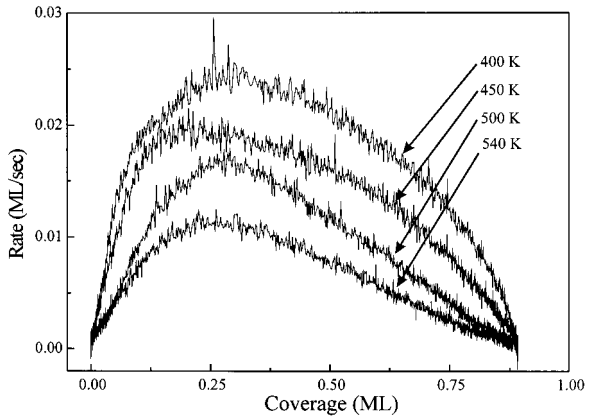

Figure 4. The CO_2 evolution rate, or oxygen removal rate, as a function of oxygen coverage for temperatures between 400 and 540 K. The data are for a CO partial pressure of 7×10^{-8} Torr and were obtained from the data in Figure 3 using eq 1. The rate is expressed in units of ML/s defined as number of oxygen atoms removed, or CO_2 molecules formed, per Pd atom on an unreconstructed Pd(100) surface.

coverage between 0 and 0.15 ML and then decreased linearly with coverage between 0.3 and 0.9 ML. At the lower temperatures, the rate depended more weakly on oxygen coverage with the rate rising rapidly at low coverages before passing through a broad maximum at 0.25 ML and then sharply rolling off above 0.75 ML. These results suggest that at high temperatures the reaction is first order in oxygen coverage at low coverages, while at high coverages oxygen blocks sites for CO adsorption. The weaker dependence on coverage at the lower temperatures can be explained in terms of a precursor mechanism. In this case, CO remains on the surface in a weakly adsorbed state long enough to either find oxygen to react with at low coverages, or find an empty adsorption site at high coverages.

If it is assumed that CO remains on oxygen-covered Pd so briefly that no CO accumulates on the surface during the experiments, then the data in Figure 4 can also be expressed in terms of reactive sticking probabilities for CO as a function of O coverage. At 7×10^{-8} Torr and 300 K the CO flux is 2.7×10^{13} cm^{-2} s^{-1}. The surface density of Pd(100) is 1.3×10^{15} cm^{-2} suggesting a maximum O removal rate of 0.020 ML/s. Figure 4, however, shows a maximum instantaneous rate of 0.023 ML/s at 400 K. The high instantaneous rate could be due to CO accumulation on the surface during the non-steady-state experiment. If this were the case, the results would depend on the CO pressure, with lower pressures making CO accumulation less likely and the maximum rate lower. Varying the CO pressure by a factor of 7, however, produced no significant change in the maximum rate per impinging CO molecule. Alternatively, the anomalously high sticking probabilities could be due to overestimates of the oxygen coverage, errors in the CO pressure measurement, or a breakdown in the assumption that the pumping speed is high enough that the reaction rate is proportional to the rise in the CO_2 pressure. Small shifts in the CO_2 baselines were observed suggesting that CO_2 accumulated in the system that would have caused the pressure rise to overstate the reaction rate. In any event, although the anomalously high reaction probability creates experimental uncertainties in the exact values of the reactive sticking coefficient, the data still clearly show trends in the reaction probability as a function of coverage.

The data for the different temperatures in Figure 4 can be used to construct Arrhenius plots for any oxygen coverage. Data for 0.3 and 0.7 ML are shown in Figure 5. At 0.7 ML, the curve is linear between 420 and 540 K before showing signs of

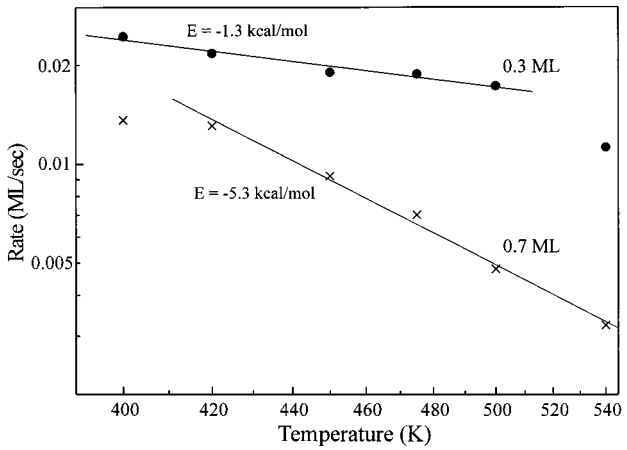

Figure 5. Arrhenius plot of the rate of CO_2 formation, or oxygen removal, versus $1/T$ for a CO partial pressure of 7×10^{-8} Torr and two different oxygen coverages. The rate data and coverages were obtained from the data in Figure 3 using eq 1. The activation energies were calculated using a linear fit to the data between 400 and 500 K for 0.3 ML and between 425 and 540 K for 0.7 ML.

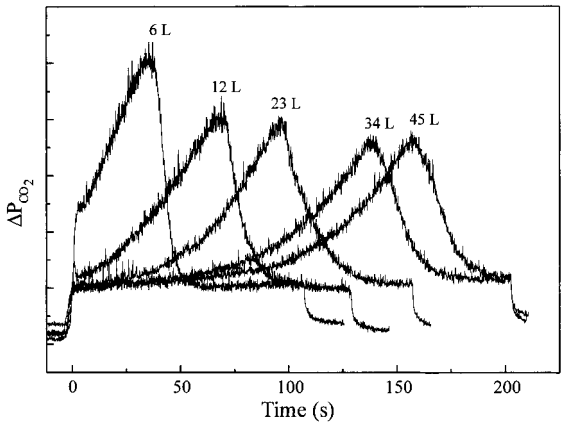

Figure 6. Plots of the rise in CO_2 partial pressure versus time for CO exposed at 7×10^{-8} Torr to Pd(100) surfaces preexposed to varying amounts of NO_2 at 500 K. All reactions were carried out at 500 K. As the NO_2 exposure dropped below 23 L, the peak heights increased and the peaks narrowed.

leveling off at 400 K. The slope of the line indicates an apparent activation energy of −5.3 kcal/mol. The rate depends less strongly on temperature at the lower coverage with an apparent activation energy of only −1.3 kcal/mol between 400 and 500 K. The rate appears to drop off more sharply with temperature above 500 K; however, the experiments were limited to 540 K because at high coverages oxygen starts to desorb just above 550 K.[16]

The reaction experiments were also performed at different initial coverages at 500 K; the results are shown in Figure 6. As expected, the lag decreases with decreasing NO_2 preexposure. There are, however, a couple of surprises in Figure 6. First, increasing the NO_2 exposure from 23 to 45 L increased the lag by over 60% even though the uptake curve in Figure 1 shows no measurable change in the oxygen coverage. In addition, Figure 6 shows that as the lag decreased, the peak became sharper and more intense. Since the pressure rise is proportional to the reaction rate, this indicates that the rate depends not only on the oxygen coverage and temperature but also on how the oxygen coverage was reached. This is not due to an experimental artifact; because of the change in the peak widths, the integrals of the curves are consistent with the coverages expected on the basis of the NO_2 exposures.

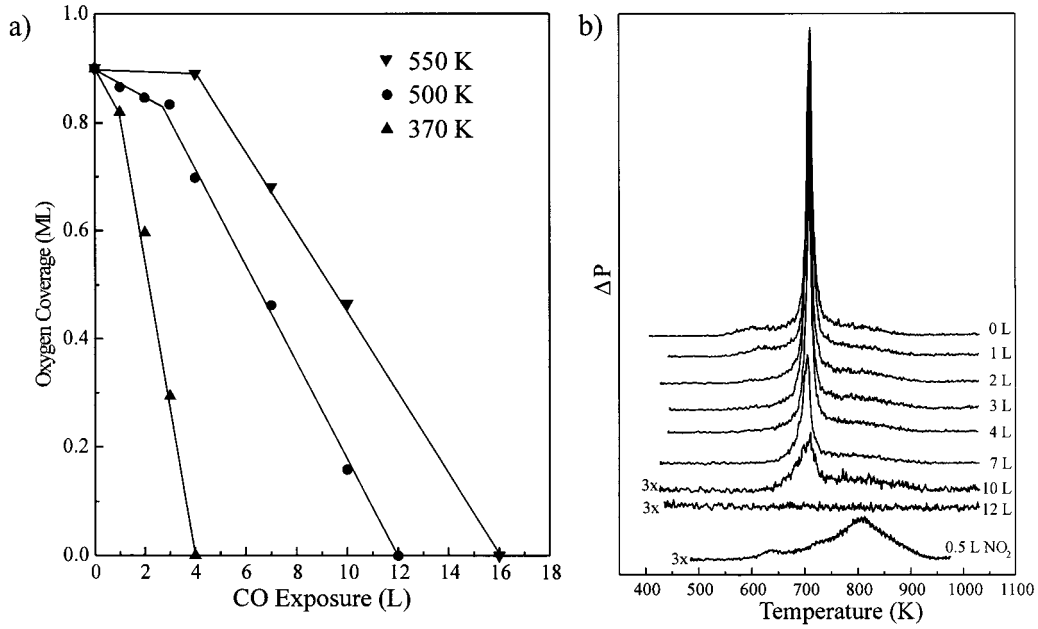

Figure 7. (a) Plots of oxygen coverage remaining on the surface versus CO exposure for surfaces preexposed to 20 L of NO_2. The data points were obtained by exposing the surface to 20 L of NO_2 at 500 K, then exposing the surface to CO at the desired temperature, and finally desorbing the remaining oxygen in a TPD experiment. Integrating the TPD curves yielded the remaining oxygen coverage. (b) Series of TPD curves obtained after dosing 20 L of NO_2 at 500 K, and then exposing the surface to varying amounts of CO at 500 K. For comparison, the bottom trace shows the TPD curve obtained after dosing 0.5 L of NO_2 at 500 K which yields an oxygen coverage of 0.17 ML.

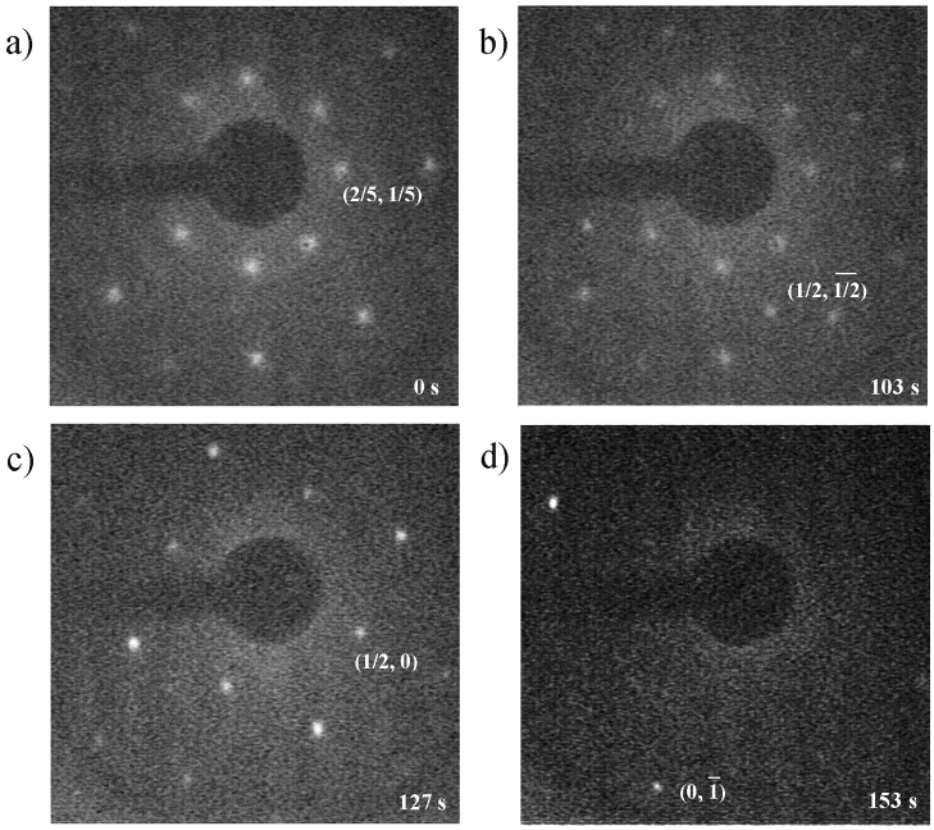

Figure 8. Series of LEED patterns extracted from a LEED movie recorded while 3×10^{-8} Torr CO was being exposed to a Pd(100) surface preexposed to 23 L of NO_2 at 500 K. The reaction was carried out at 490 K. Recording was started roughly 10 s after the CO pressure was increased. The electron energy was 44 eV. (a) ($\sqrt{5} \times \sqrt{5}$)R27° pattern of the starting surface. (b) After 103 s the (1/2,1/2) spots became visible. (c) Only a (2×2) pattern was seen after 127 s. (d) After 153 s the (1×1) of the clean surface was restored.

The reaction of CO with oxygen-covered Pd(100) was also studied by exposing oxygen-covered surfaces to varying amounts of CO and then measuring the amount of oxygen left on the surface using TPD. During these experiments, no CO or CO_2 could be detected indicating that CO did not stay on the surface. The results are plotted in Figure 7a as remaining oxygen coverage versus CO exposure for surfaces preexposed to 20 L of NO_2 at 500 K. The data again show that the initial reduction

rate is very slow, that following the incubation period oxygen is rapidly removed from the surface, and that the rate is higher at lower temperatures. More interestingly, Figure 7b shows the O_2 TPD curves for 500 K. In addition to the two O_2 desorption features seen in Figure 2, Figure 7b shows a weak peak at 600 K that has previously been assigned to PdO dissociation.[15,16] Figure 7b shows that by 2−3 L CO exposure the bulk oxide peak was gone. Since this coincides with the point where the reduction rate begins to accelerate, this suggests that the lag in CO_2 production is associated with the presence of bulk oxide on the surface. As more oxygen was removed, Figure 7b shows that the intensity of the two remaining peaks decrease in concert. Even after 10 L of CO exposure decreased the coverage to 0.16 ML, the 700 K peak remained far more intense than the 800 K peak. In contrast, when the same coverage was reached by exposure to 0.5 L of NO_2 at 550 K, the peak intensities were reversed with the 800 K peak dominating. In addition, when oxygen is adsorbed on Pd(100) the sharp desorption peak shifts to higher temperature as the coverage is increased,[16,20] while Figure 7b shows no change in the peak temperature when oxygen is removed from the surface. Thus the TPD results indicate that the oxygen left on the surface following reduction of oxidized Pd at 500 K can be bound in a different state than oxygen adsorbed from the gas phase, even though the coverage may be the same. This helps explain the sensitivity of the reduction rate to the surface history.

c. Surface Phase Transitions Monitored Using LEED. To characterize the phase transitions that occur during reduction of oxygen-covered Pd(100) surfaces, LEED movies were recorded during exposure to CO. Figure 8a−d shows four frames extracted from a LEED movie recorded at 490 K with 3×10^{-8} Torr CO. Initially, the surface exhibited the ($\sqrt{5} \times \sqrt{5}$)R27° pattern (Figure 8a). After 103 s, Figure 8b shows additional spots at the (1/2,1/2) positions signaling the formation of (2 × 2) phases. With increasing exposure the ($\sqrt{5} \times \sqrt{5}$)R27° pattern disappeared and was replaced by a (2 × 2) pattern (Figure 8c) and then finally by the (1 × 1) pattern of the clean surface (Figure 8d). These results indicate that although a (5 × 5) pattern can be observed prior to the ($\sqrt{5} \times \sqrt{5}$)R27° pattern when the surface is oxidized,[16,21,20] when oxygen is removed from the ($\sqrt{5} \times \sqrt{5}$)R27° structure by reaction with CO the surface decays directly to the (2 × 2) phases.

The kinetics of the phase transitions can be characterized by plotting the intensities of the spots characteristic of the different structures as a function of time; such a plot is shown in Figure 9a. In this graph, the (2/5,1/5) spots track the ($\sqrt{5} \times \sqrt{5}$)R27° structure, the (1/2,0) spots the p(2 × 2) structure, the (1/2,1/2) spots the p(2 × 2) and c(2 × 2) structures, and the (1,0) spots the bare surface. Although the (1,0) spots are common to all the structures, the short electron mean free path at 44 eV caused these spots to be very weak for the oxygen-covered phases. Consistent with the CO_2 evolution, Figure 9a exhibits a lag before the LEED pattern changes. As the disappearance of the ($\sqrt{5} \times \sqrt{5}$)R27° accelerated, the intensity of the (1/2,1/2) and (1/2,0) spots rapidly increased. When the intensity of the ($\sqrt{5} \times \sqrt{5}$)R27° pattern approached zero, the intensity of the spots associated with the (2 × 2) structures leveled off and then plummeted while the (1 × 1) pattern of the bare surface rapidly intensified.

The (1/2,1/2) spots are common to the p(2 × 2) and c(2 × 2) structures while the (1/2,0) spot is only seen for the p(2 × 2) structure. As shown in Figure 9b, when the spot intensities are normalized to their maximum intensities, it becomes apparent that the (1/2,1/2) spots intensifed before the (1/2,0) spots suggesting that the c(2 × 2) structure appeared before the p(2 × 2) structure. The stronger intensity of the (1/2,1/2) spots, however, should not be taken as an indication that the surface contains more of the c(2 × 2) structure. When the surface was prepared by dosing 10 L of O_2 at 370 K which populates only the p(2 × 2) structure,[16,24] at 44 eV the (1/2,1/2) spots were also more intense than the (1/2,0) spots. In the remainder of this paper, (2 × 2) will be used to denote surfaces that may contain both p(2 × 2) and c(2 × 2) domains.

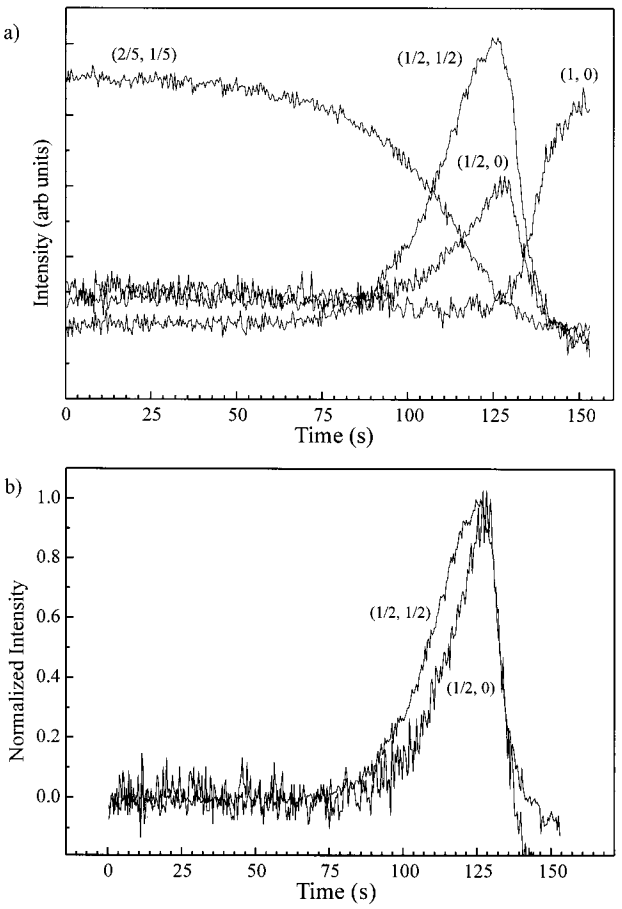

Figure 9. (a) LEED spot intensities versus time calculated from the movie shown in Figure 8. The (2/5,1/5) spots were used to follow the ($\sqrt{5} \times \sqrt{5}$)R27° structure, the (1/2,0) spots the p(2 × 2) structure, the (1/2,1/2) spots the p(2 × 2) and c(2 × 2) structures, and the (1,0) spots the (1 × 1) bare surface structure. The data were obtained by averaging over all equivalent spots. (b) Plot of the intensity of the (1/2,1/2) and (1/2,0) spots normalized to their maximum intensities. The graph shows that the (1/2,1/2) spots intensified first suggesting that the c(2 × 2) structure preceded the p(2 × 2) structure as the surface was reduced.

Comparing Figures 3, 4, and 9 clearly suggests that the increase in the rate that follows the lag is due to the buildup of highly reactive (2 × 2) phases at the expense of the unreactive PdO(001)-like reconstructed layer. Comparing the figures also suggests that at the higher temperatures the rate builds up linearly as the (2 × 2) regions spread across the surface. This can be understood simply in terms of the reaction rate being proportional to the surface area of the more reactive sites. The nonlinear dependence on coverage at the lower temperatures again suggests a precursor mechanism in which CO can weakly adsorb on less reactive ($\sqrt{5} \times \sqrt{5}$)R27° areas and then migrate to the (2 × 2) regions and react which would cause the reaction rate to depend less strongly on the area of the more reactive sites.

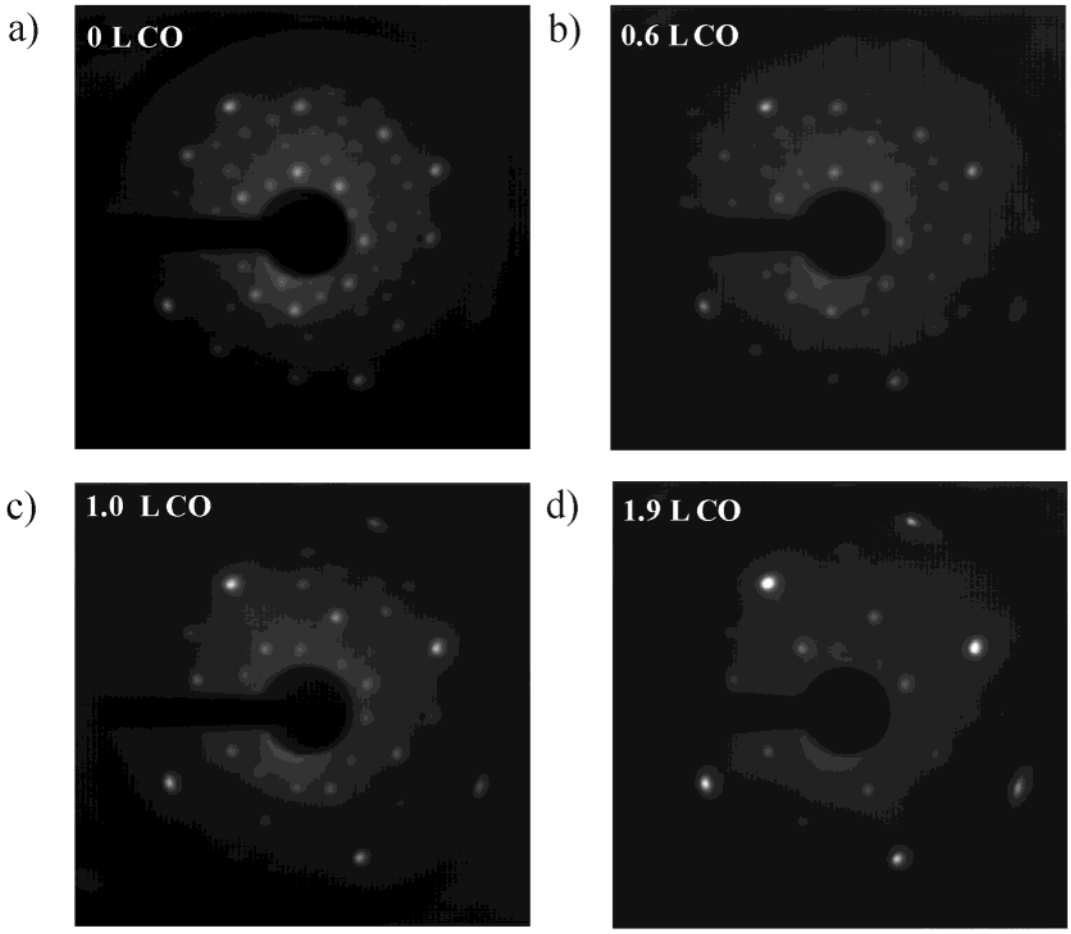

Figure 10. LEED patterns obtained after exposing a surface that contained a mixture of (5 × 5) and ($\sqrt{5} \times \sqrt{5}$)R27° domains to varying amounts of CO. (a) The starting surface, (b) after exposure to 0.6 L of CO the (5 × 5) pattern faded, (c) after exposure to 1.0 L of CO see a (2 × 2) pattern and the ($\sqrt{5} \times \sqrt{5}$)R27° pattern, (d) after 1.9 L of CO only the (2 × 2) pattern was visible. The electron energy was 63 eV.

Previous studies have shown that the formation of the (5 × 5) structure is very sensitive to surface preparation.[16,20] Therefore, to test whether the surface bypassed the (5 × 5) structure in Figure 8 because of an inability to form that structure, a (5 × 5) surface was prepared and then exposed to O_2 so that the (5 × 5) and ($\sqrt{5} \times \sqrt{5}$)R27° patterns were observed simultaneously. This surface was then reacted with CO at 465 K; the lower temperature was selected because the (5 × 5) pattern converts to the other patterns with time at 500 K. The starting surface is shown in Figure 10a. The (2/5,1/5) and (4/5,2/5) spots are common to the (5 × 5) and ($\sqrt{5} \times \sqrt{5}$)R27° patterns and so the high intensity of these spots indicates that the surface contained ($\sqrt{5} \times \sqrt{5}$)R27° domains. After exposure to 0.6 L of CO at 465 K, Figure 10b shows that all the 1/5 order spots dimmed except those associated with the ($\sqrt{5} \times \sqrt{5}$)R27° structure while the (1/2,1/2) and (1/2,0) spots intensified. Thus reaction with CO has removed oxygen from the (5 × 5) domains converting them into (2 × 2) domains. As shown in Figure 10c, increasing the CO exposure to 1.0 L removed any traces of the (5 × 5) pattern while the ($\sqrt{5} \times \sqrt{5}$)R27° remained clear. By 1.2 L of CO the 1/5 order spots were difficult to see and the surface displayed the (2 × 2) pattern shown in Figure 10d. At no point did any of the 1/5 order spots intensify indicating that reaction of the ($\sqrt{5} \times \sqrt{5}$)R27° structure with CO does not convert it into the (5 × 5) structure. Further, the rapid disappearance of the (5 × 5) pattern prior to the ($\sqrt{5} \times \sqrt{5}$)-R27° pattern indicates that the (5 × 5) structure is highly reactive toward CO.

d. Surface Phase Transitions Monitored Using STM. The changes that occur as oxygen-covered Pd(100) surfaces react with CO were observed on the nanometer scale by recording STM movies during reaction at elevated temperatures. Figure 11 shows the starting surface for one such movie. The wide range image in Figure 11a shows that the terraces contain two distinct levels with an apparent height difference of 0.08 nm, much less than the 0.19 nm Pd(100) step height. The higher resolution image in Figure 11b shows that the lower levels are characterized by a striped structure. The stripes are rotated 27° with respect to Pd[011] and their spacing is within experimental error of $\sqrt{5}$ times the Pd atom spacing on the (100) surface. Previously, we showed that the striped appearance is typical of the ($\sqrt{5} \times \sqrt{5}$)R27° structure and thus the lower or darker gray levels display the ($\sqrt{5} \times \sqrt{5}$)R27° structure.[16] Although the structure of the upper level could not be resolved, images of surfaces prepared in the same manner indicate that the raised levels display (2 × 2) structures.[16] In Figure 11 the surface was in the third stage of oxidation described in the Introduction, and thus the (2 × 2) areas contain additional oxygen, possibly in subsurface sites. To distinguish this surface from the adsorbed overlayers at coverages less than 0.5 ML, in the remainder of this paper this state will be referred to as "high-density (2 × 2)". The small white protrusions in the images are due to Si impurities that are brought to the surface and oxidized when the crystal is exposed to oxidants.[16] Their presence does not impact the surface chemistry.

The sequence of STM images in Figure 12 illustrate what

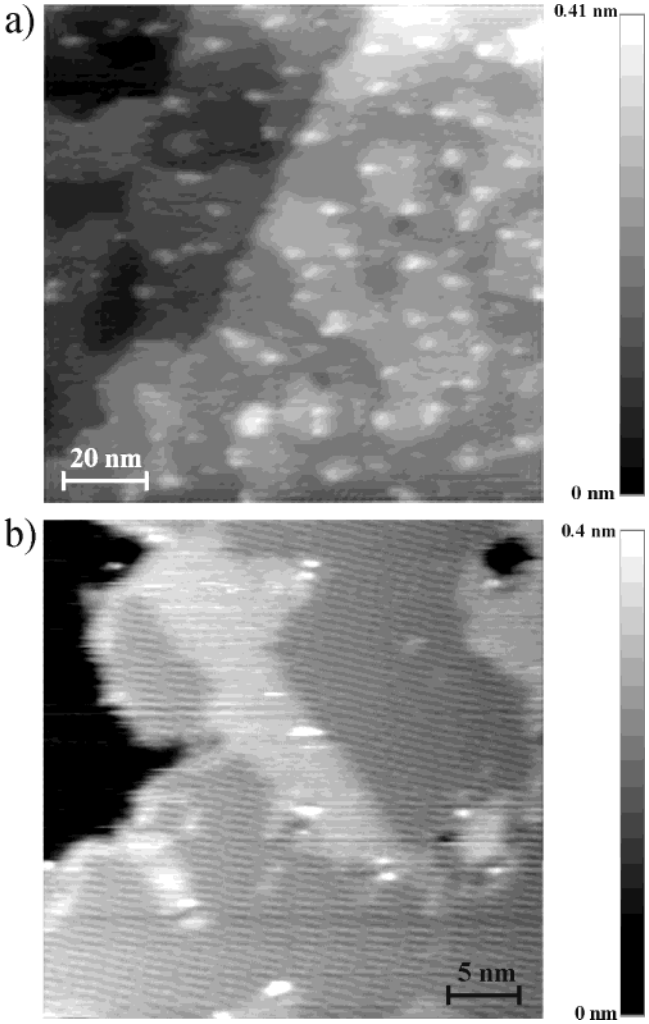

Figure 11. STM images of Pd(100) obtained during in situ O_2 exposure at 500 K. (a) Wide range image showing two distinct levels on each of the terraces. (b) Higher resolution image reveals a striped structure on the lower level. The stripes are 0.16 nm high and their orientation and spacing are consistent with the $(\sqrt{5} \times \sqrt{5})R27°$ structure. The images were obtained at 1 V sample bias and 0.5 nA tunneling current.

happened when the surface in Figure 11 was exposed to 2×10^{-9} Torr CO at 500 K while maintaining an O_2 pressure of 5×10^{-8} Torr. The images show that no changes in the step edges occurred as the lower $(\sqrt{5} \times \sqrt{5})R27°$ areas slowly shrank with time. Only when the $(\sqrt{5} \times \sqrt{5})R27°$ structure was completely removed did the steps begin to recede to their original positions. The last few images show this process was comparatively very fast, so fast that oxygen was kept in the chamber to slow this step so that it could be followed with STM. Because O_2 adsorbs much more rapidly on the (2×2) phases than on the $(\sqrt{5} \times \sqrt{5})R27°$ phase, the background oxygen also masked the increase in the reduction rate observed with LEED and mass spectrometry as the area of the high-density (2×2) domains increased.

To test the reversibility of the reduction process the CO was turned off before reduction was complete and the O_2 pressure was increased to 1.9×10^{-7} Torr while continuing to record an STM movie. As shown in Figure 13, frames from this movie show that the reduction process is completely reversible. In the beginning of the movie the terraces rapidly regrew. The lower level that corresponds to the $(\sqrt{5} \times \sqrt{5})R27°$ structure only appeared after terrace growth stopped.

The STM movies also provide insight into the interconversion between surface oxygen phases. The kinetic and LEED data indicate that the $(\sqrt{5} \times \sqrt{5})R27°$ phase is far less reactive toward CO than the (2×2) and (5×5) phases. Therefore, in Figure 12 the reaction took place primarily on the raised high density (2×2) areas. Still, no changes in the step structure were observed until after the $(\sqrt{5} \times \sqrt{5})R27°$ domains were completely removed from the terraces indicating that the high-density (2×2) areas did not change as long as $(\sqrt{5} \times \sqrt{5})$-R27° domains were present. Thus, as oxygen is removed from the high-density (2×2) areas it must be rapidly replenished by oxygen from neighboring $(\sqrt{5} \times \sqrt{5})R27°$ domains. Removing oxygen from the $(\sqrt{5} \times \sqrt{5})R27°$ domains converts them into high-density (2×2) domains. When the $(\sqrt{5} \times \sqrt{5})$-R27° domains are exhausted, the reaction decreases the coverage in the high-density (2×2) domains causing the terraces to collapse back to their original dimensions.

IV. Discussion

The results reveal that reduction of oxidized Pd(100) surfaces by CO proceeds as follows. Carbon monoxide reacts only very slowly with the PdO(001)-like $(\sqrt{5} \times \sqrt{5})R27°$ reconstructed surface. When CO is exposed to a surface entirely covered by the $(\sqrt{5} \times \sqrt{5})R27°$ phase, there is a lag before any CO_2 can be detected. Small increases in the oxygen coverage that create PdO greatly increase the lag indicating that PdO is even less reactive toward CO, and that O removed from $(\sqrt{5} \times \sqrt{5})$-R27° domains is replenished by neighboring PdO clusters preventing their reduction into more reactive lower coverage phases. It is otherwise difficult to explain how such small amounts of PdO can so profoundly affect the progress of the reaction; if PdO was reactive it would be rapidly removed and thus would not affect the lag in CO_2 production. Once all the PdO is removed, reaction on the $(\sqrt{5} \times \sqrt{5})R27°$ domains converts them into high-density (2×2) domains thought to contain subsurface oxygen. These domains are much more reactive and so the rate accelerates as patches of this structure build up on the surface. Oxygen transport between $(\sqrt{5} \times \sqrt{5})$-R27° domains and neighboring high-density (2×2) domains is rapid and so as long as any $(\sqrt{5} \times \sqrt{5})R27°$ domains are present, the reaction does not decrease the oxygen content of the high density (2×2) domains. At 500 K and above, the reaction rate increases linearly with the area of the more reactive domains while at lower temperatures the rate accelerates more quickly. This effect can be understood in terms of a longer CO lifetime on the $(\sqrt{5} \times \sqrt{5})R27°$ domains at the lower temperature allowing sufficient time for diffusion to the reactive domains. Once the $(\sqrt{5} \times \sqrt{5})R27°$ domains are completely exhausted, the high-density (2×2) structure collapses and the terraces and islands that grew when it was formed shrink. The CO_2 production rate then drops as oxygen is depleted from the surface.

The temperature dependence of the reaction rate provides insight into why the more oxidized surface phases are less reactive toward CO. Decreases in reaction rate with temperature can be readily understood in terms of Langmuir−Hinshelwood models. In this case, at high temperatures and low pressures the reaction is limited by the low coverage, or short lifetime, of one of the reactants on the surface. As the temperature increases, the lifetime decreases more rapidly than the surface reaction rate increases, resulting in a drop in the overall reaction rate. The greater drop-off in the rate at higher oxygen coverages can be due to either a lower activation energy for the surface reaction step at high coverages, or the high oxygen coverage decreasing the CO heat of adsorption which would cause the reaction rate to fall more severely at lower temperatures. The

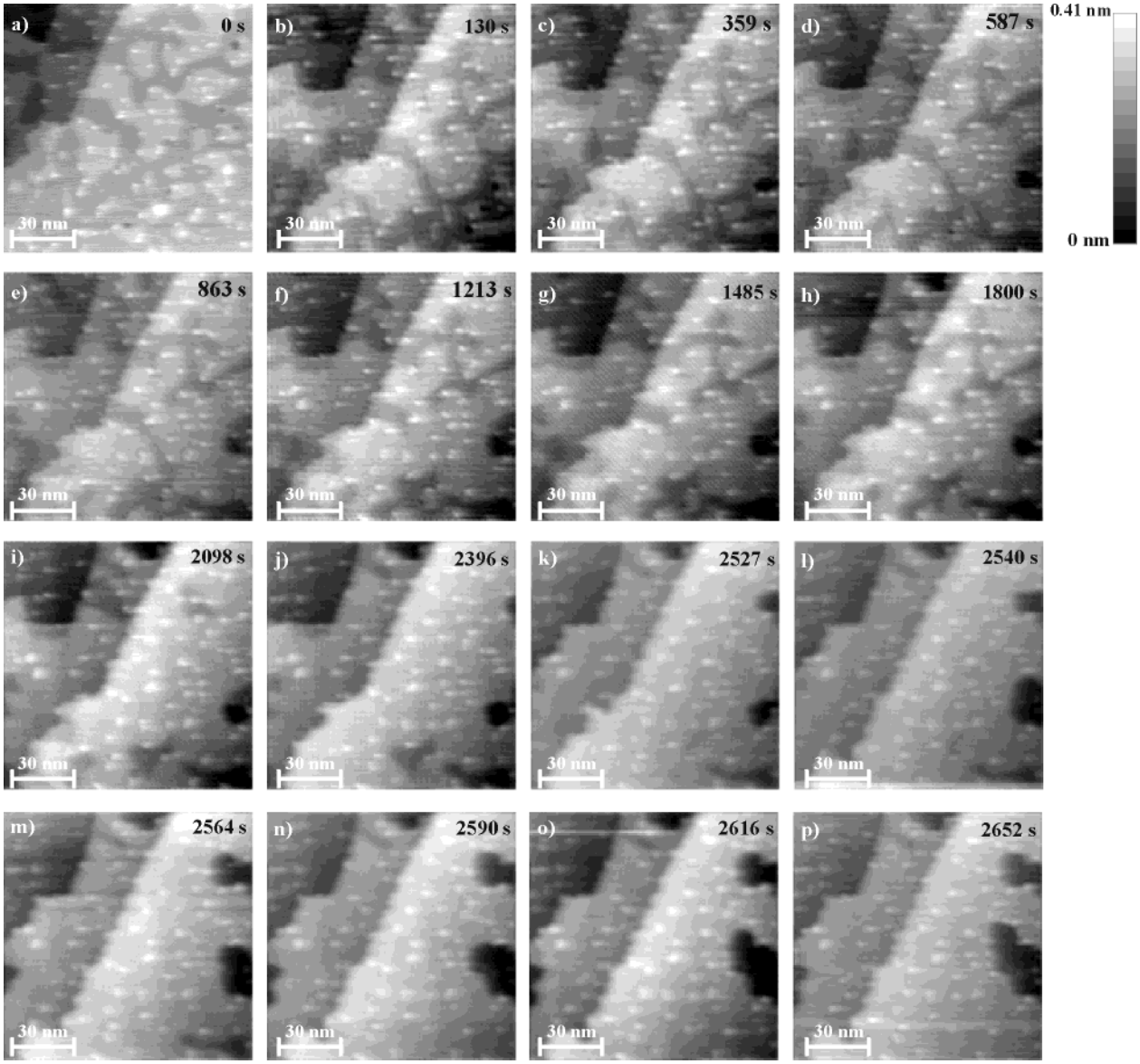

Figure 12. Frames extracted from an STM movie recorded while a Pd(100) surface was being exposed to 5×10^{-8} Torr O_2 and 2×10^{-9} Torr CO at 500 K. Prior to starting the movie the oxygen coverage was built up by exposing the surface to higher oxygen pressures with no CO in the chamber. At $t = 0$ s, CO was admitted into the chamber. The images were recorded using a 2.0 V sample bias and a tunneling current of 0.5 nA.

TPR data in Figure 2b suggest that no CO_2 forms at or below 335 K when the surface reconstructs, and set a lower bound of 375 K for the CO_2 reaction peak on the reconstructed surface versus 400 K for the p(2 × 2) overlayer. Thus there is no evidence that the activation energy for the surface reaction step is substantially reduced at high coverage. Therefore it is concluded that the low reactivities of the ($\sqrt{5} \times \sqrt{5}$)R27° surface and PdO are due to the inability of these surfaces to strongly adsorb CO.

The sensitivity of the reaction rate to not only the oxygen coverage but also to how that oxygen coverage is reached may be explained in terms of nucleation of the surface phases that can create a hysteresis in the coverage at which the phase transitions occur. For example, when the oxygen coverage is increased by adsorption, the ($\sqrt{5} \times \sqrt{5}$)R27° structure may first be observed when the (2 × 2) phases are saturated. When the oxygen coverage is decreased by reaction with CO, this can initially introduce vacancies into the ($\sqrt{5} \times \sqrt{5}$)R27° structure which are observed in STM images.[16] The vacancy concentration may exceed the thermodynamic limit before the (2 × 2) phases nucleate in a manner analogous to supersaturation of the vapor phase prior to condensation. As a result, for a given oxygen coverage, the fraction of the surface covered by the ($\sqrt{5} \times \sqrt{5}$)R27° structure can be lower when the oxygen coverage is increasing versus when the coverage is decreasing. Since the ($\sqrt{5} \times \sqrt{5}$)R27° structure is much less reactive, this would cause the reactivity to be lower when the coverage is decreasing. The same arguments apply to the other phase transitions. This explanation is consistent with the TPD results that show a different population of the desorption peaks when the oxygen coverage is increased by adsorption versus decreased by reaction with CO.

Regardless of the origin of the sensitivity of the reaction rate to the surface history, the results suggest that under more practical, higher pressure conditions that CO oxidation rates over Pd(100) will display hysteresis when the oxygen pressure is increased and decreased. Specifically, the rates will be higher as the oxygen pressure is increased through the range where the ($\sqrt{5} \times \sqrt{5}$)R27° structure covers the surface and PdO begins to form than when the pressure is decreased and PdO and the

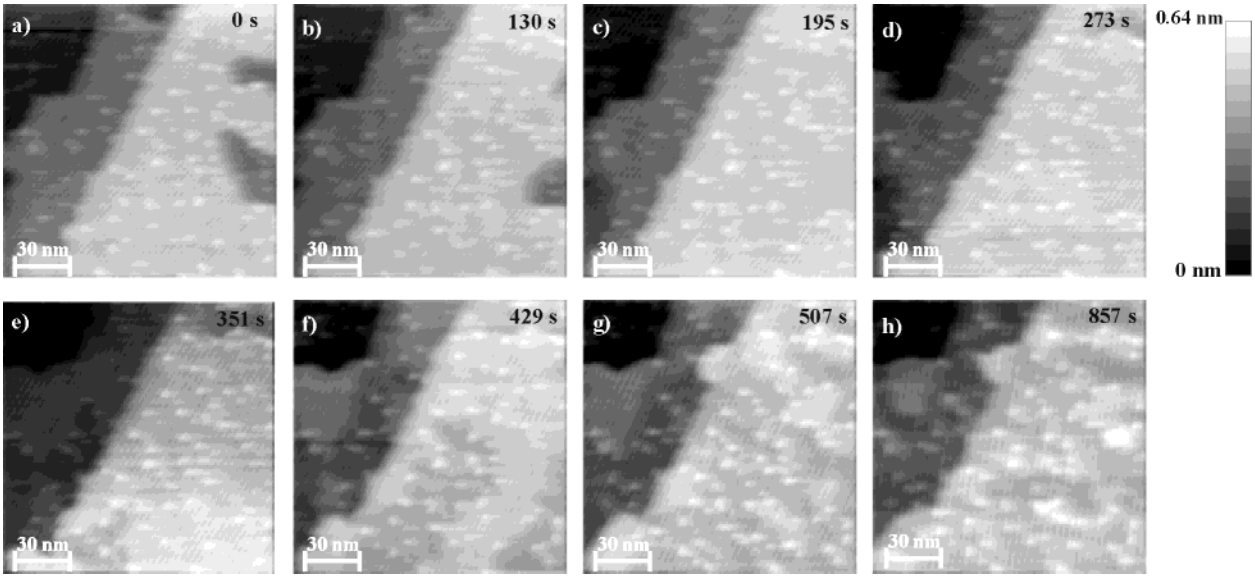

Figure 13. Series of images taken from an STM movie of the same area of the surface shown in Figure 11 after shutting off the CO and increasing the O_2 pressure to 2×10^{-7} Torr O_2 at 500 K. The images were obtained using a 2 V sample bias and 0.5 nA tunneling current.

($\sqrt{5} \times \sqrt{5}$)R27° structure dissociate. This result can help explain the observed sensitivity of Pd oxidation catalysts to the catalyst history.[5,7,8,12,13]

V. Summary

Oxygen can exist in as many as six different states on Pd(100): (1) a p(2 × 2) overlayer; (2) a c(2 × 2) overlayer; (3) a high density (2 × 2) state that may include subsurface oxygen; (4) a (5 × 5) reconstructed surface; (5) a PdO(001)-like ($\sqrt{5} \times \sqrt{5}$)R27° reconstruction; and (6) bulk PdO. Temperature-programmed reaction studies showed that the c(2 × 2) overlayer is the most reactive toward CO, producing CO_2 below 335 K while the other oxygen phases produced CO_2 between 375 and 405 K. Isothermal reaction measurements showed that the ($\sqrt{5} \times \sqrt{5}$)R27° and PdO surfaces are relatively unreactive toward CO. In contrast, the (5 × 5) phase was as reactive as the (2 × 2) phases. At all oxygen coverages, the reduction rate decreased with increasing temperature over the range studied.

Low energy electron diffraction and in situ elevated-temperature STM were used to follow the structural changes that occurred as the surfaces were reduced. Together with the kinetic measurements, the results indicated that the reactivity of the surface increased as unreactive ($\sqrt{5} \times \sqrt{5}$)R27° domains were replaced by (2 × 2) domains. Further, the results indicated that oxygen transport between PdO, the ($\sqrt{5} \times \sqrt{5}$)R27° structure, and the (2 × 2) phases is fast. As a result, reaction on ($\sqrt{5} \times \sqrt{5}$)R27° domains does not convert them into high density (2 × 2) areas until all the neighboring PdO is removed, and the high density (2 × 2) areas are not reduced until the ($\sqrt{5} \times \sqrt{5}$)R27° structure is completely removed.

Acknowledgment. The authors thank D. Ciuparu and L.D. Pfefferle for their insight into Pd-catalyzed oxidation reactions. The authors also acknowledge the assistance of W. Gao, H. L. Chan, R. E. Tanner, and M. Li in carrying out this work. This research was supported by the Petroleum Research Foundation of the American Chemical Society under Grant ACS-PRF-34181-AC5.

References and Notes

(1) Sekiba, T.; Kimura, S.; Yamamoto, H.; Okada, A. *Catal. Today* **1994**, *22*, 113.

(2) Shinjoh, H.; Muraki, H.; Fujitani, Y. *Appl. Catal.* **1989**, *49*, 195.

(3) Tagliaferri, S.; Koppel, R. A.; Baiker, A. *Appl. Catal., B: Environmental* **1998**, *15*, 159.

(4) Farrauto, R. J.; Hobson, M. C.; Kenelly, T.; Waterman, E. M. *Appl. Catal., A: General* **1992**, *81*, 227.

(5) Lyubovsky, M.; Pfefferle, L. D. *Appl. Catal. A: General* **1998**, *173*, 107.

(6) Lee, J. H.; Trimm, D. L. *Fuel Proc. Technol.* **1995**, *42*, 339.

(7) Lyubovsky, M.; Pfefferle, L. D. *Catal. Today* **1999**, *47*, 29.

(8) Lyubovsky, M.; Pfefferle, L.; Datye, A.; Bravo, J.; Nelson, T. *J. Catal.* **1999**, *187*, 275.

(9) Ladas, S.; Imbihl, R.; Ertl, G. *Surf. Sci.* **1989**, *219*, 88.

(10) Bassett, M. R.; Imbihl, R. *J. Chem. Phys.* **1990**, *93*, 811.

(11) Bondzie, V.; Kleban, P.; Browne, D. A. *J. Vac. Sci. Technol. A* **1993**, *11*, 1946.

(12) Furuya, T.; Sasaki, K.; Hanakata, Y.; Mituyasu, K.; Yamada, M.; Tsuchiya, T.; Furuse, Y. Proceedings of the Second International Workshop on Catalytic Combustion, 1994, Tokyo, Japan.

(13) McCarty, J. G.; Wong, V. L.; Chang, Y. F. *Scr. Metall. Mater.* **1994**, *31*, 1115.

(14) Bondzie, V. A.; Kleban, P.; Dwyer, D. J. *Surf. Sci.* **1996**, *347*, 319.

(15) Zheng, G.; Altman, E. I. *Surf. Sci.* **2000**, *462*, 151.

(16) Zheng, G.; Altman, E. I. *Surf. Sci.*, in press.

(17) Voogt, E. H.; Mens, A. J. M.; Gijzeman, O. L. J.; Geus, J. W. *Surf. Sci.* **1997**, *373*, 210.

(18) Banse, B. A.; Koel, B. E. *Surf. Sci.* **1990**, *232*, 275.

(19) Orent, T. W.; Bader, S. D. *Surf. Sci.* **1982**, *115*, 323.

(20) Chang, S.-L.; Thiel, P. A. *J. Chem. Phys.* **1988**, *88*, 2071.

(21) Chang, S.-L.; Thiel, P. A.; Evans, J. W. *Surf. Sci.* **1988**, *205*, 117.

(22) He, J.-W.; Norton, P. R. *Surf. Sci.* **1988**, *204*, 26.

(23) Vu, D. T.; Mitchell, K. A. R.; Warren, O. L.; Thiel, P. A. *Surf. Sci.* **1994**, *318*, 129.

(24) Stuve, E. M.; Madix, R. J.; Brundle, C. R. *Surf. Sci.* **1984**, *146*, 155.

(25) Logan, A. D.; Paffett, M. T. *J. Catal.* **1992**, *133*, 179.

(26) Szanyi, J.; Goodman, D. W. *J. Phys. Chem.* **1994**, *98*, 2972.

(27) Nakakura, C. Y.; Phanse, V. M.; Zheng, G.; Bannon, G.; Altman, E. I.; Lee, K. P. *Rev. Sci. Instrum.* **1998**, *69*, 3251.

(28) Nakao, F. *Vacuum* **1975**, *25*, 431.

(29) King, D. A. *Surf. Sci.* **1975**, *47*, 384.